Proc. Nat. Acad. Sci. USA
Vol. 68, No. 11, pp. 2802–2805, November 1971

Flicker Responses in Monkey Lateral Geniculate Nucleus and Human Perception of Flicker

(de Lange characteristics/microelectrodes/macaques/single cells/critical flicker frequency)

H. SPEKREIJSE*, D. VAN NORREN, AND T. J. T. P. VAN DEN BERG*

Institute for Perception TNO, Kampweg 5, Soesterberg, The Netherlands

Communicated by Floyd Ratliff, September 2, 1971

ABSTRACT **An analysis was made of the impulse discharge patterns—evoked by sinusoidal luminance modulation—of single cells in the lateral geniculate nucleus of the macaque monkey. The goal was to determine whether a correspondence could be observed between flicker detection by human subjects in psychophysical experiments and electrophysiological measurements of discharge patterns of single cells of the lateral geniculate nucleus. We found that the average discharge patterns of single cells exhibited the following behavior when mean retinal illumination was changed: In the low-frequency region (less than about 10 Hz) the response strength (impulses/sec) is independent of the mean luminance, in accordance with Weber's law; in the high-frequency region (above about 10 Hz) the response depends on the absolute modulation amplitude, in accordance with the Ferry-Porter law. Therefore the main features of human critical flicker frequency data are already present in the cellular (lateral geniculate nucleus) response of the macaque monkey. However, the steepness of the high frequency fall-off in the response characteristics of these cells is much less than the corresponding fall-off in the human critical-flicker-frequency curves.**

It was de Lange (1–3) who introduced the harmonic analysis approach that underlies present day understanding of much of the chaotic literature (4) about flicker perception. He (2) demonstrated that the high-frequency flicker threshold does not depend on the waveform of the flickering light provided that the amplitude of the fundamental Fourier component of this waveform was held constant. The fruitfulness of Fourier analysis in the study of flicker perception under scotopic conditions had already been indicated by Ives (5) in 1922, but the full potential of harmonic analysis only became evident after de Lange's extensive study at photopic levels of illumination (6–8).

De Lange's contribution stems from his separation of the effects of luminance change and mean luminance. He was able to separate these effects by using modulated light rather than the classical on/off square-wave stimulus. As an example of luminance modulation at a constant mean luminance, a sinusoidal modulating waveform is depicted in the insert of Fig. 1. The two important stimulus parameters are the average luminance L_0, and the amplitude of the luminance modulation A, which can be controlled independently of L_0. For a given average luminance, L_0, de Lange plotted the threshold modulation m ($m = A/L_0$) as a function of frequency on logarithmic scales. Examples of such curves of flicker sensitivity versus frequency (de Lange curves) are given in Fig. 1. These psychophysical data were obtained for a human subject under the same stimulus conditions as those with which the animal experiments described in this paper were performed. The curves illustrate the extreme steepness of the fall-off in human flicker sensitivity for frequencies above 10 Hz.

With the particular aim of accounting for the extremely sharp attenuation of the de Lange curves in the high-frequency region, models have been proposed that are made up of as many as ten cascaded temporal integration or RC-elements (9–14). If these N-stage integrator models are applied to human flicker sensitivity, then the problem arises of deciding how these elements are distributed along the visual pathway. In order to answer this question, we studied in monkey the impulse discharge patterns evoked by sinusoidal luminance modulation in single lateral geniculate cells. We chose macaques for our experiment since these monkeys are almost ideal animals for investigations of the relations between psychophysical data (in man) and single-unit activity. Behavioral experiments have shown that not only their wavelength discrimination function, but also their photopic and scotopic spectral-sensitivity functions, resemble those of man (15–17). Moreover, recent electroretinographical (18) measurements indicate an identity—except for a slight deviation for wavelengths below 450 nm—between the photopic spectral sensitivities of man and macaque.

METHODS

2-3 kg macaques (*Macaca mulatta* and *Macaca speciosa*) were maintained under light nembutal anaesthesia (10 mg/kg per hr) throughout the experiments, which lasted 15–20 hr. The monkeys were held in a stereotaxic instrument. The eyelids were retracted and the pupils dilated. The sclera of each eye was sutured to the stereotaxic instrument so as to prevent spontaneous eye movements. The single-cell activity in the lateral geniculate nucleus (LGN) was recorded with 3 M KCl-filled micropipettes with resistances of 5–20 MΩ. The electrodes were lowered through a trephine hole in the skull. In order to improve the signal-to-noise ratio, the shaped impulse responses were averaged by a computer of average transients (CAT). The number of summations triggered by the periodic light stimulus was generally 50–600, depending upon the discharge rates. A final record of the impulse density distribution was obtained by plotting the analogue output of the computer with an X-Y recorder.

Abbreviation: LGN, lateral geniculate nucleus.

* Present address: Laboratory of Medical Physics, University of Amsterdam, Herengracht 196, Amsterdam, The Netherlands.

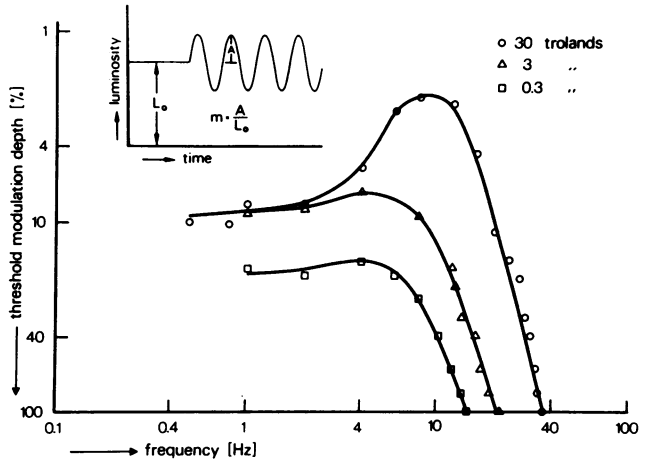

FIG. 1. Modulation depth for flicker fusion in man as a function of frequency. White, sinusoidally modulated light is used at three different average retinal illuminations: 30, 3, and 0.3 trolands. The Maxwellian field subtended 15° of visual angle. *Insert:* The intensity of a sinusoidal light stimulus is depicted as a function of time. The unmodulated stimulus, of intensity L_0, changes at a given moment into a sinusoidal modulated light with amplitude A. The depth of modulation is conveniently expressed by the parameter $m = A/L_0$. The stimulus frequency is f(Hz). The mathematical representation of the waveform is $X(t) = L_0 (1 + m \sin 2\pi ft)$.

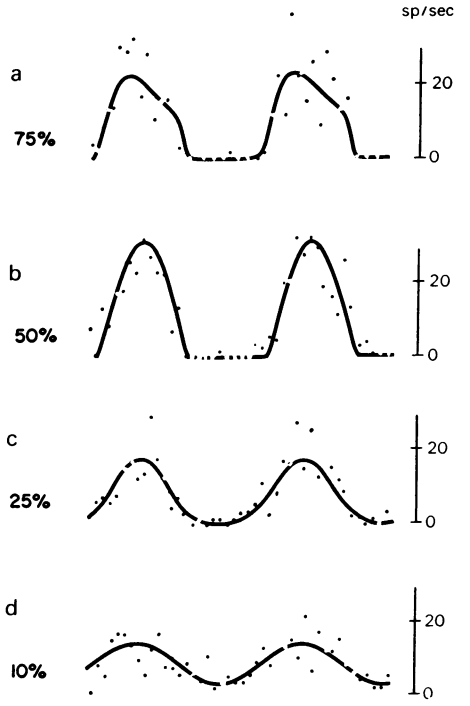

FIG. 2. Average impulse responses of the excitatory component of a green$^+$–red$^-$ LGN cell are given as a function of the modulation depth of a 8-Hz sinusoidally modulated light. For relatively weak stimuli (*c* and *d*), the density distribution of the impulses has roughly the same shape as the sinusoidal stimulus. For higher modulation depths (*a* and *b*), distortion becomes evident. The number of summations is 100; the mean retinal illumination amounts to 480 trolands.

The optical system consisted of three separate pathways combined through a beam splitter. One channel contained interference filters, neutral-density filters, and an electrical shutter (rise time, 2 msec). The second channel provided a chromatic adaptation light with adjustable intensity. The final beam, containing an aperture stop that could be varied in size and position, was focused in the plane of the pupil of either eye of the animal, so as to present the monkey with a Maxwellian field that subtended up to 15° of visual angle. This apparatus was used to classify the various LGN impulse discharges on the basis of their color coding.

In order to facilitate comparisons of our results with previous work, and in particular with the extensive pioneering studies of Russell L. DeValois, we followed the DeValois method* (19) of data reduction.

Once a unit had been isolated and classified by DeValois' procedure, the first beam was replaced by a third beam, which allowed the unit to be stimulated with modulated waveforms at a constant average luminance. The light source that generated this third beam was a television projection tube (Philips MW 6/2); its modulated output was monitored and controlled by a photocell (20).

RESULTS

On the basis of their responses to different stimulus wavelengths the LGN cells can be divided into two classes. These are: (*a*) cells that show either excitation or inhibition of the spontaneous activity for all stimulus wavelengths, and (*b*) cells that show an inhibition to stimulus wavelengths at one end of the spectrum, and excitation to wavelengths at the other end of the spectrum. These two cell types have been

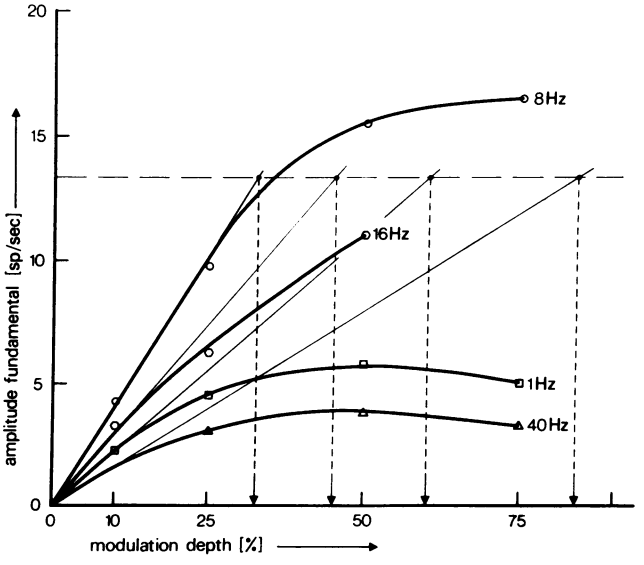

FIG. 3. This figure gives the amplitude of the fundamental component of the averaged discharge pattern of the excitatory component of a green$^+$–red$^-$, LGN cell to sine-wave modulated light of various frequencies. Only for extremely-low modulation depths is the amplitude of the average response proportional to the strength of the input sine wave. The mean retinal illumination is about 480 trolands.

* This method consisted of recording the responses to light flashes of one second in duration. The number of impulses in the one second periods directly preceding, during and after the cessation of the light flash were counted.

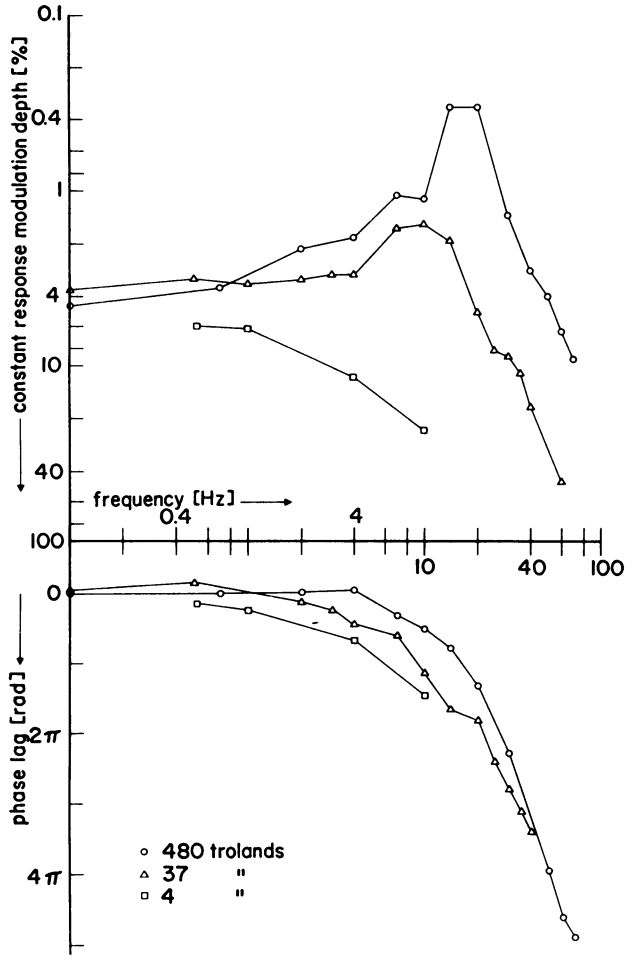

FIG. 4. Amplitude (*above*) and phase (*below*) characteristics of a yellow$^-$–blue$^+$ LGN cell determined with blue, sinusoidally-modulated light at three different retinal illuminations (480, 37, 4 troland). The amplitude characteristics (de Lange curves) are obtained by plotting the modulation depth required for each stimulus frequency to reach a constant response of 8.6 impulses/sec.

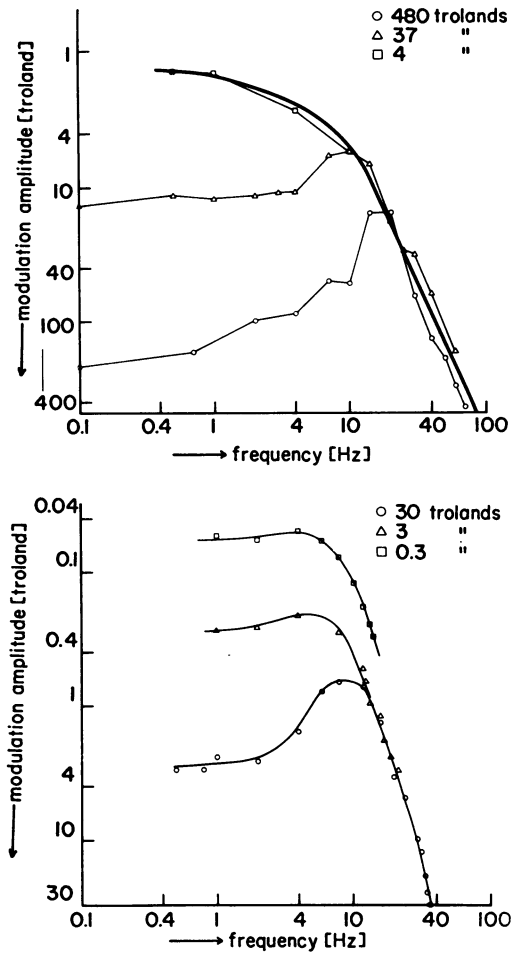

FIG. 5. Absolute modulation amplitude, mL_0, at flicker fusion in a human psycho-physical experiment and at constant response of a monkey LGN cell (*top*), as a function of frequency. The top-half data are replotted from Fig. 4, the bottom-half data are obtained from Fig. 1. It should be noted that in contrast to the flicker-fusion data, the values at the vertical axis of the monkey data largely depend on the arbitrarily chosen constant-response criterion. The mean retinal illuminations of the sinusoidal stimuli are given in the figures.

called by DeValois (19) *non-opponent* and *opponent* cells. The action spectrum of opponent cells has only one neutral point; i.e., only one wavelength can be found that does not produce any change in firing rate. Depending on the location of this neutral point, the opponent cells can be classified (21) as red–green and yellow–blue cells.

In our experiments, we first determined the color coding of a particular LGN cell. Sinusoidally modulated light with a color coinciding with one of the peaks in the action spectrum was then used as a tool to investigate the impulse discharges as a function of frequency and modulation depth. Examples of average responses to an 8-Hz sinusoidally modulated light are illustrated as a function of modulation depth in Fig. 2. This figure shows that for relatively weak stimuli (Fig. 2 *c* and *d*), the density distribution of the nerve impulses has roughly the same shape as the sinusoidal stimulus. However, at higher modulation depths the average responses exhibit such nonlinear behavior as saturation on the one hand and clipping (zero spike frequency) on the other hand (Fig. 2 *a* and *b*).

We have derived the de Lange curves from plots of the fundamental component in the average responses versus modulation depth. Fig. 3 gives such plots for a range of frequencies of the constant-luminance sine-wave stimulus. The tangents (straight lines in Fig. 3) were drawn through the origin of these curves, and the intersections of these tangents with some convenient constant threshold criterion (13 spikes/sec in Fig. 3) were determined. Next, the modulation depths required to reach this criterion were plotted as a function of stimulus frequency†. We used de Lange's convention of plotting the ordinate with increasing modulation downwards, so as to emphasize similarities between these curves and the attenuation chracteristics of electronic systems.

The top of Fig. 4 shows a set of de Lange curves deter-

† It should be noted that the choice of the threshold criterion is of no influence upon the shape of the de Lange characteristics. The threshold criterion sets the amplitude characteristic along the vertical axis; the tangent lines determine the shape.

mined for a yellow$^-$–blue$^+$ cell, stimulated with a blue light at three different retinal illuminations (480 trol, 37 trol, and 4 trol‡). Two conclusions emerge directly from this figure: (*a*) At the low-frequency end, the flicker threshold is independent of the mean luminance and solely determined by the modulation depth. This shows the applicability of the Weber law in this frequency range. (*b*) For frequencies above about 10 Hz, the LGN cells become increasingly more sensitive as luminance is raised.

The bottom half of Fig. 4 gives the phase characteristics that belong to the de Lange curves just described. These characteristics demonstrate an increased phase lag between the stimulating sinusoid and the fundamental component in the average response as stimulus frequency increases. This phase lag seems compatible with the shapes of the electrophysiological de Lange curves.

Ten other cells, both opponent and non-opponent, recorded by us in this investigation, show in general the same features as depicted for the particular cell in Fig. 4. However, the behavior at the low-frequency end of the de Lange characteristic is not always as independent of the mean luminance as for the cell presented. But even for cells dissimilar to that shown in Fig. 4, two regions can be distinguished: a low-frequency one in which the threshold is mainly determined by the modulation depth, and a high-frequency one in which the sensitivity increases with luminance.

DISCUSSION

Kelly (22) and also Levinson and Harmon (7) have proposed that an envelope can be obtained for the de Lange curves by plotting the absolute threshold amplitude, mL_0, rather than the critical modulation depth, m, as a function of frequency. Fig. 5 shows two sets of modulation sensitivity curves, replotted in luminance amplutude only, without regard to the adaptation level. In the top half of this figure, the data of Fig. 4 are replotted; the bottom half gives the replotted data of Fig. 1. The data of Fig. 1 were obtained for a human subject under the same stimulus conditions as those of the animal experiment. The similarity between the two sets of data is evident. In both conditions the high-frequency data join—within limits§—together in a common envelope. Anywhere along this envelope, the high-frequency threshold depends on the absolute and *not* on the relative modulation amplitude, in accordance with the well-known Ferry-Porter law. The major difference between the two sets of data is the steepness of the high-frequency fall-off. Whereas this fall-off in psychophysical data may reach values as high as 60 dB/octave (1), we never observed such high values in our LGN data; in the case shown, the attenuation amounts only to 12 dB/ octave. Since this is the only relevant difference between the two sets of data, our experimental findings indicate directly that the main features of the de Lange characteristics are already present in the lateral geniculate response. Therefore, assuming that the behavioral de Lange characteristics in monkey prove to be comparable to those of man, it may be that further stages do no more than add to the high-frequency fall-off.

‡ It should be noted that the same troland value, because of the smaller nodal distance of the monkey eye, represents a higher retinal illumination in the monkey eye than in the human eye.

§ As Kelly (8) has pointed out, a common envelope holds only within a restricted—but still large—range of retinal illuminations. For retinal illuminations less than about 0.1 troland or higher than about 9000 trolands, the replotted de Lange curves deviate from a common envelope.

We are grateful to P. Padmos, M.Sc. for allowing us to use his equipment, and for giving us advice necessary to carry out the experiments. We are greatly indebted to Mrs. N. H. Blokland for her technical assistance.

1. de Lange, H., Ph.D. thesis, Technological University, Delft (1954).
2. de Lange, H., *J. Opt. Soc. Amer.*, **44**, 380 (1954).
3. de Lange, H., *J. Opt. Soc. Amer.*, **48**, 777, and 784 (1958).
4. Landis, C., *An Annotated Bibliography of Flicker Fusion Phenomena* (Armed Forces-National Research Council, Univ. Michigan, 1953).
5. Ives, H. E., *J. Opt. Soc. Amer. Rev. Sci. Instrum.*, **6**, 254 (1922).
6. Levinson, J., *Science*, **130**, 919 (1959).
7. Levinson, J., and L. D. Harmon, *Kybernetik*, **1**, 107 (1961).
8. Kelly, D. H., *Doc. Ophthalmol.*, **18**, 16 (1964).
9. De Voe, R. D., *Doc. Ophthalmol.*, **18**, 128 (1964).
10. Campbell, F. W., and J. G. Robson, *Doc. Ophthalmol.*, **18**, 83 (1964).
11. Fuortes, M. G. F., and A. L. Hodgkin, *J. Physiol. (London)*, **172**, 239 (1964).
12. Sperling, G., *Doc. Ophthalmol.*, **18**, 3 (1964).
13. Marimont, R. B., *J. Physiol. (London)*, **179**, 489 (1965).
14. Pinter, R. B., *J. Gen. Physiol.*, **49**, 565 (1966).
15. DeValois, R. L., and J. H. Jacobs, *Science*, **162**, 533 (1968).
16. Schrier, A. M., and D. S. Blough, *J. Comp. Physiol. Psychol.*, **62**, 457 (1966).
17. Sidley, M. A., and G. H. Sperling, *J. Opt. Soc. Amer.*, **57**, 816 (1967).
18. van Norren, D., *Vision Res.*, in press.
19. DeValois, R. L., I. Abramov, and J. H. Jacobs, *J. Opt. Soc. Amer.*, **56**, 966 (1966).
20. Denier van der Gon, J. J., J. Strackee, and L. H. van der Tweel, *Phys. Med. Biol.*, **3-2**, 164 (1958).
21. DeValois, R. L., J. H. Jacobs, and I. Abramov, *Science*, **146**, 1184 (1964).
22. Kelly, D. H., *J. Opt. Soc. Amer.*, **49**, 730 (1961).